

# Glass Melting Tanks as Models for the Behavior of Mantle

By

Masanaga Kunugi\* and Katsuaki TAKAHASHI\*\*

(Received August 3, 1970)

The authors have attempted to make clear the characteristics of convection current of molten glass in a cross-fired glass tank furnace by model techniques and also obtained some information about flow patterns of natural convection motion in mantle.

In this paper we introduce an outline of our study on the model experiments in glass tank furnace<sup>1)</sup> and try to obtain some information about their analogy with mantle flow.

## I. Studies on the Flow of Molten Glass in a Glass Tank by Model Techniques.

In continuous glass manufacturing processes batch is gradually melted in a tank furnace, whose function is to serve as a chamber for the chemical reactions of the batch components, and also to serve as a container of the molten glass giving sufficient time for refining and conditioning. On the other hand the tank may be regarded as a heat transfer system in which the top of the molten glass serves as the heat receiving surface, while the side and bottom walls act as heat discharging surfaces as shown in Fig. 1. Between these surfaces heat is carried partly by conduction and radiation and partly by the circulation of hot molten glass, so that the phenomena occurring in a glass tank furnace, i.e., melting the batch, refining and conditioning the molten glass, and other chemical and physical processes are connected inseparably with the convection current of molten glass.

Unfortunately there are few data published of direct measurements, such as the temperature distribution and flow velocity in actual tank furnaces.

Therefore, to make clear the fundamental characteristics of convection current the authors carried out the model experiments under conditions satisfying as far as possible the law of similarity.

---

\* Department of Industrial Chemistry

\*\* Department of Industrial Chemistry, Okayama University

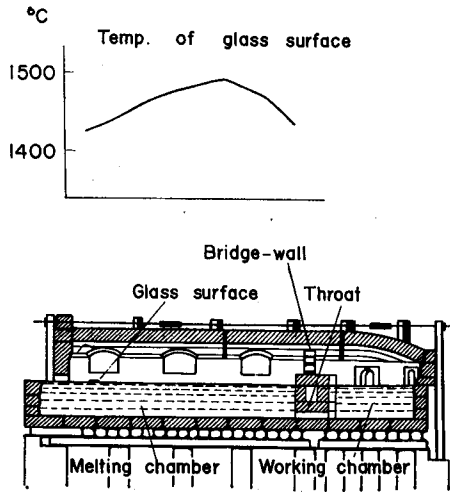


Fig. 1. Cross-fired glass tank

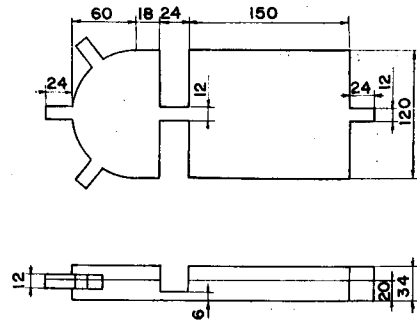


Fig. 2. Dimensions of model tank in mm

A model of glass tank was made from transparent plates of plastics to the scale 1/50. Its dimensions are given in Fig. 2. Molten glass was replaced by 82% glycerin. The melting chamber of tank was covered by a number of hot plates encased in a metal sheath, the temperatures of the plates could be controlled independently in order to get the desired temperature distribution in the longitudinal direction. As for the similarity between actual tank and model we

Table 1. Experimental conditions and values of physical constants for glycerin and glass

Item	Glass	Glycerin	Symbols
Temperature at spring Surface, °C	1480	54	$\theta_1$
Bottom, °C	1325	32	$\theta_2$
Glass surface temp. at bridge-wall, °C	1430	47	
Average velocity of fluid in the tank for pull rate 80t/day, cm/min	0.40	0.063	$v$
Density, g/cm <sup>3</sup>	2.287(1388°C)	1.201 (41°C)	$\rho$
Viscosity, g/cm·sec	110( " )	0.24 ( " )	$\mu$
Kinematic Viscosity $\mu/\rho$ , cm <sup>2</sup> /sec	48( " )	0.20 ( " )	$\nu$
Coefficient of volume expansion	$5.3 \times 10^{-5}$	$5 \times 10^{-5}$	$\beta$
Thermal conductivity cal/sec·dm·°C	0.15 (1388°C)	$6.8 \times 10^{-4}$	$\lambda$
Specific heat, cal/g·°C	0.3	0.58	$C_p$
$Re = du/v$	0.0108	0.0105	$d = \text{depth of glass}$
$Pr = C_p \mu / \lambda$	120	140	
$Gr = \{d^3(\theta_1 - \theta_2)\beta g\} / \nu^2$	3200	1900	

satisfied this with an agreement between the three principal numbers, namely the Reynolds, the Prandtl, and the Grashof numbers for two sets of temperatures as given in Table 1. The experimental conditions and the physical constants are summarized in the same table.

The temperature distributions in the model liquid were determined with Cu-Constantan thermocouple. For example, the isothermal lines in the model liquid are shown in Fig. 3, together with those of the corresponding furnace. The flow patterns were observed from the photographic records of the tracks of tracer plastic spheres coated with aluminium powder moving in the illuminated area of the liquid.

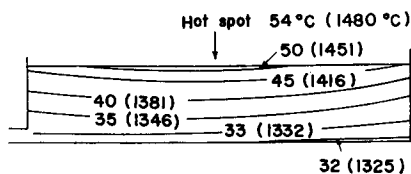


Fig. 3. Temperature distributions in models. In parentheses temperatures converted to actual tank are shown

## 1. General Flow Pattern of Convection Current.

### (a) Convection current; no pull.

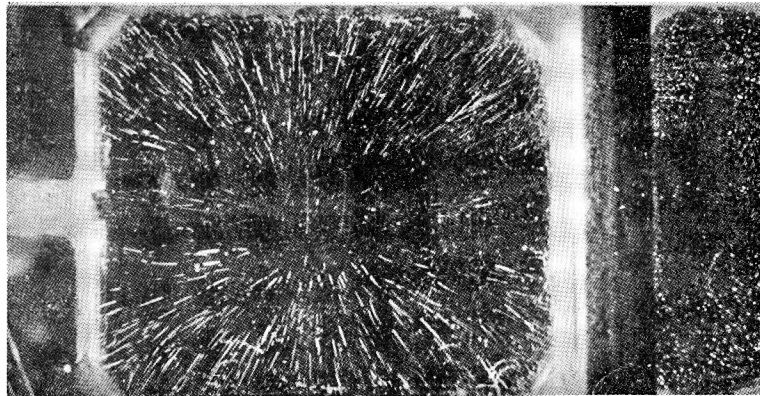
The simplest case of our argument is that of the convection current in the fluid contained in a box.

Fig. 4 shows the typical flow patterns of the liquid in the melting chamber of the 1/50 scale model of a tank when no pull is applied, in which a) reproduces the surface current, b) the flow in the vertical surface along the longitudinal centerline, c) the rapid downward stream near the wall and d) the pattern in a plane intermediate between the wall and the hot spot.

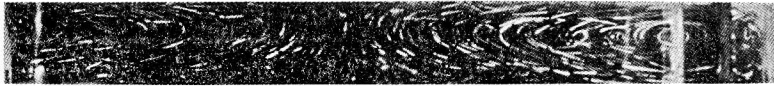
Fig. 4a indicates clearly that the convection currents are spreading radially from the spot toward the walls. Fig. 4b shows that the surface currents flow at first toward the walls, then change direction to flow rapidly towards the bottom and finally flow back towards the hot spot. In the last stage the moving liquid receives heat from above becoming lighter and lighter through the increase in temperature and rises gradually toward the surface until the liquid gushes out like a spring at the centre.

A glance at the picture will show that the flow pattern consists of innumerable concentric closed curves whose common centre is located near the wall.

Comparing Fig. 4c and 4d, it will be clear that there exists a thin layer along the walls in which the liquid flows very rapidly. This is an important potential source for the driving force of the convection current occurring in the confined space, whereas in an infinitely extending fluid, the driving force is the difference of the



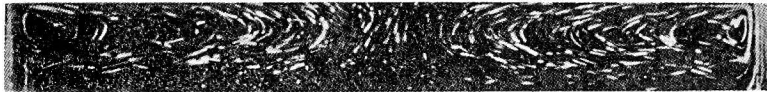
a. Surface current



b. Flow in the vertical plane along the longitudinal centerline



c. Downward stream near the wall



d. Flow in a plane intermediate between the hot spot and the wall

Fig. 4. Typical flow patterns of convection current in the melting chamber of a 1/50 scale model of tank

pressure between any two points.

Finally it should be noted that in the layer near the walls as well as at the centre of the hot spot the liquid flows vertically up and down showing that the horizontal component of the velocity is negligible.

As for velocity of flow the velocity distribution in the vertical section along the longitudinal center line is given in Fig. 5.

(b) Convection superposed on the pull current.

We observed the flow pattern in the same model, but operating it at the pull rate corresponding to  $6 \text{ ft}^2/\text{ton, day}$  in the actual tank. It will be seen that the horizontal velocity is increased by the pull, but no radical change of flow pattern is caused by this pull.

Fig. 6 shows a perspective schematical drawing in order to make the picture

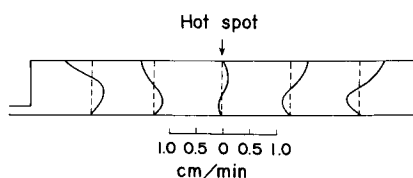


Fig. 5. Velocity distribution in the vertical section along the longitudinal center line.

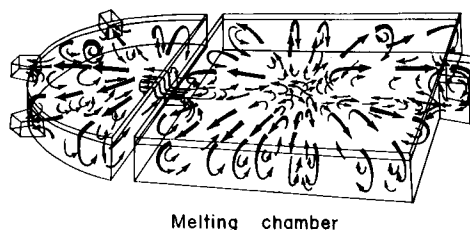


Fig. 6. Schematic drawing of the convection currents

clear. The thicker arrows represent the currents which are closer to the surface.

## II. Model Experiment Illustrating the Convection Current in Mantle.

We are now going to touch briefly upon the model experiment illustrating the convection current in mantle.

To study flow patterns of natural convective motion in a viscous fluid medium bounded by two spherical surfaces for different temperature distributions the model experiment was carried out. The viscous material in mantle was replaced by 99.4% glycerin. The spherical model immersed in a thermostat which was kept at 25°C. To satisfy the conditions of similitude for the flow we considered the Grashof number and the Prandtl number. The dimensions of model, the experimental conditions and the physical constants for mantle and glycerin are given in Table 2. The physical constants of glycerin given in the Table are corresponding values for

Table 2. Experimental conditions and values of physical constants for mantle and glycerin

Item	Mantle	Glycerin	Glycerin/ $\epsilon$ Mantle
Temp. difference, $(\theta_1 - \theta_2), ^\circ\text{C}$	1100	5	
Density, $\rho, \text{g/cm}^3$	4.91	1.26	0.26
Viscosity, $\mu, \text{g/cm}\cdot\text{sec}$	$3 \times 10^{22}$ $3.7 \times 10^{13}$	8.4	$2.8 \times 10^{-21}$ $2.3 \times 10^{-13}$
Coefficient of volume expansion, $\beta, 1/^\circ\text{C}$	$4.2 \times 10^{-5}$	$5 \times 10^{-5}$	$1.2 \times 10$
Specific heat, $C_p, \text{cal/g}\cdot^\circ\text{C}$	0.3	0.58	1.93
Thermal conductivity, $\lambda, \text{cal/sec}\cdot\text{cm}\cdot^\circ\text{C}$	$2 \times 10^{-3}$	$6.8 \times 10^{-4}$	$3.4 \times 10^{-1}$
Depth of convection cell, $d, \text{cm}$	$2.8 \times 10^8$	3.2	$1.1 \times 10^{-8}$
$Gr$	$2.7 \times 10^{-17}$ 1.81	1.81	$0.67 \times 10^{17}$ 1.0
$Pr$	$4.5 \times 10^{24}$ $5.6 \times 10^{15}$	$7.2 \times 10^3$	$1.6 \times 10^{-21}$ $1.3 \times 10^{-12}$

temperature  $\theta_1=30^\circ\text{C}$  and  $\theta_2=25^\circ\text{C}$  where  $\theta_2$  and  $\theta_1$  are the temperatures of upper and lower spherical surfaces respectively as shown in Fig. 7.

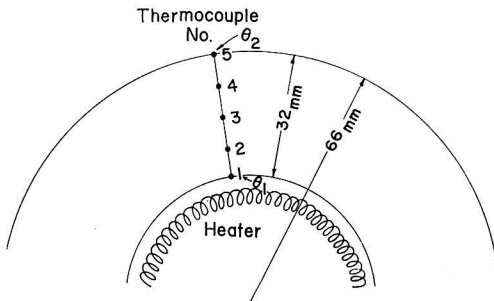


Fig. 7. Schematical drawing of model

If we choose  $\mu=3.7 \times 10^{13}$  for viscosity of mantle,  $Gr$  and  $Pr$  are 1.81 and  $5.6 \times 10^{15}$  respectively.

Fig. 8~Fig. 10 reproduce the flow patterns of the model liquid bounded by two spherical surfaces for different radial temperature gradients. Figures tell us about the general patterns of recirculating current. The velocity of flow can be determined by the track of particle photographed in the Figure. The velocity of convection current in mantle can be calculated by  $\epsilon_v = \epsilon_\mu \cdot \epsilon_{Re} / \epsilon_d \cdot \epsilon_\rho$  where  $\epsilon_\mu$ ,  $\epsilon_{Re}$ ,  $\epsilon_d$ ,  $\epsilon_\rho$  and  $\epsilon_v$  are the ratio of physical constants or values for actual mantle and model liquid. The suffixes  $\mu$ ,  $Re$ ,  $d$ ,  $\rho$  and  $v$  correspond respectively to the values

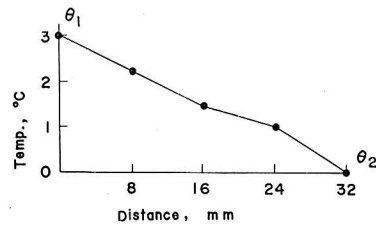
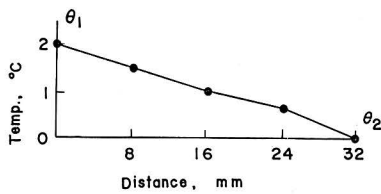


Fig. 8. Flow pattern of convection current ( $\theta_1 - \theta_2 = 2^\circ\text{C}$ )



Fig. 9. Flow pattern of convection current ( $\theta_1 - \theta_2 = 3^\circ\text{C}$ )

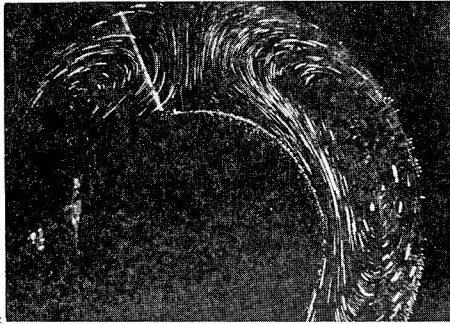
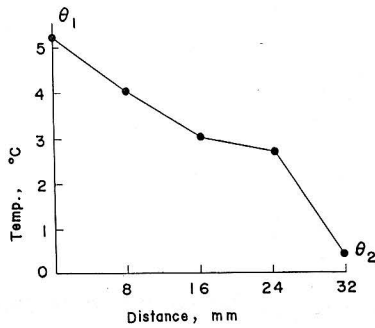


Fig. 10. Flow pattern of convection current  
( $\theta_1 - \theta_2 = 5^\circ\text{C}$ )

of viscosity, Reynolds number, depth of cell, density and velocity.

In our experiment we have many bold assumptions and oversimplifications, especially, the effective direction of gravity is vertical, which is not the case in an actual mantle. With the aid of carefully planned experiments on models it is possible with such a experimental method to simulate the phenomena in mantle and to obtain clear cut pictures of convection current. However, in order to agree the conditions of similarity between mantle and model liquid with each other it is necessary to use more viscous liquid for model liquid, for example, Polybutene (Furukawa HV-300,  $\mu = 1000$  poise at  $30^\circ\text{C}$ ) and use a smaller scale model.

#### References

- 1) Masanaga Kungi, Katsuaki Takahashi and Ikutaro Sawai: J. Ceram. Assoc. Japan, **68** (2) 67-78 (1960)